Hindawi
Adsorption Science & Technology
Volume 2023, Article ID 7369027, 17 pages
https://doi.org/10.1155/2023/7369027

Research Article

Preparation of Breadfruit Leaf Biochar for the Application of Congo Red Dye Removal from Aqueous Solution and Optimization of Factors by RSM-BBD

M. Laxmi Deepak Bhatlu,[1] **P. S. Athira**,[2] **Neethu Jayan**,[3] **Debabrata Barik**,[4] **and Milon Selvam Dennison**[5]

[1]*Department of Chemical Engineering, KPR Institute of Engineering and Technology, Coimbatore, Tamil Nadu 641407, India*
[2]*Buckman Laboratories (India) Pvt. Ltd., Chennai, Tamil Nadu 600031, India*
[3]*Department of Chemical Engineering, Texas Tech University, Lubbock, TX 79409, USA*
[4]*Department of Mechanical Engineering, Karpagam Academy of Higher Education, Tamil Nadu 641021, India*
[5]*Department of Mechanical Engineering, Kampala International University, Western Campus, Kampala, Uganda 20000*

Correspondence should be addressed to M. Laxmi Deepak Bhatlu; dbhatlu.rs.che@itbhu.ac.in, Debabrata Barik; debabrata93@gmail.com, and Milon Selvam Dennison; milon.selvam@kiu.ac.ug

Received 16 November 2022; Revised 24 January 2023; Accepted 2 February 2023; Published 16 February 2023

Academic Editor: Lingzhi Yang

In this work, biochar produced from breadfruit leaves was utilized to remove the toxic Congo red dye. XRD, FTIR, and FESEM-EDX were implemented to characterize the biochar. Response surface methodology (RSM) and the Box-Behnken design (BBD) techniques were used to evaluate Congo red's optimum adsorption efficiency. The adsorption of Congo red was studied by varying dye concentrations (5–50 mg/L), times (30–240 min), pH (6–9), and dosages (0.5–2 g/100 mL). X-ray diffractometer results show that the structure of biochar is amorphous. The biochar exhibited unbounded OH, aliphatic CH group, and C=O stretch, as shown by the band peaks at 3340 cm^{-1}, 2924 cm^{-1}, and 1625 cm^{-1} intensities. RSM-BBD design results showed maximum removal efficiency of 99.96% for Congo red at pH 6.37, dye concentration 45 mg/L, time 105 min, and dosage 1.92 g, respectively. The adsorption of Congo red by biochar was successfully modeled using the Langmuir model and pseudo-second-order model. The biochar produced from breadfruit leaves exhibited a high adsorption capacity of 17.81 mg/g for Congo red adsorption. It suggests that the adsorption is both homogenous monolayer and physicochemical.

1. Introduction

The usage of dyes by several sectors harms the environment since these substances are extremely hazardous and nonbiodegradable [1]. In the dyeing industry worldwide, 30–60 liters of water are used for every kilogram of fabric colored, and enormous volumes of wastewater are discharged during the process [2]. Many pollutants and toxins from industrial wastewater contribute to global warming. Additionally, because the industrial sector requires vast amounts of water, it produces wastewater that contains both mineral and organic toxins. It is now one of the most polluting industries, even though there have been a lot of efforts to clean up the processes over the last 30 years [3, 4]. Water scarcity, rising effluent disposal expenses, and tighter discharge laws have made wastewater treatment necessary. The wide range of contaminants in water needs a variety of treatment procedures to remove them from the water that is both successful and technologically and economically viable [5].

At present, the main methods utilized for the treatment of wastewater containing dyes are carried out by chemical (chemical oxidation, coagulation, photolysis, zero-valent metal reduction, and so on), physical (membrane filtration, sedimentation, flocculation, adsorption, filtration, ion exchange, and so on), or biological approaches [6, 7]. On the other hand, the chemical approach may degrade colors

into tiny compounds with increased carcinogenic or poisonous properties by dissolving the bivalent bond of dye chromophores. While bacteria degrade biodegradable substances in biological techniques, residues of microorganisms in nonbiodegradable waste sludge are discharged into the environment and cause additional difficulties. Physical adsorption is the most effective method for removing dyes from wastewater since it produces few harmful by-products and has a wide range of material sources, while also having cheap cost, quick kinetics, and easy operation and being recyclable [8, 9]. Adsorption is the process of eliminating and recovering hazardous substances from liquids or gases by adsorbing them onto a solid surface [10–12]. Because of their great effectiveness and versatility in separating a broad variety of chemical components, adsorption methods offer the potential to remove organics from water [13]. Many studies have shown the usage of materials like walnut husk [14], composites [15], biochars from crop residues [16], natural clinoptilolite [17], sesame hull [18], the biomass of penicillium YWO1 [19], natural zeolite [20], cross-linked succinyl chitosan [21], modified bentonite [22], eucalyptus barks [23], modified attapulgite [24], clay material [25, 26], activated carbon [27], dehydrated beet pulp carbon [28], and polyurethane foam [29] as adsorbent for removal of dyes from the effluent. In addition to the above, there are a variety of man-made and naturally occurring materials that can be used in the development of sorbents, including polymeric resins, zeolites, agricultural solid waste such as date pits and fly ash, and biodegradable materials like chitosan and fungi or bacterial biomass.

Particularly, biomass-activated carbon is advised as a powerful and affordable adsorbent. This is because of its ease of use, efficacy, and capacity to remove any type of color from wastewater [30, 31]. Some of the qualities that have biomass-activated carbon an ideal adsorbent for the treatment of dye-contaminated wastewater are good size distribution, abundant functional groups, and wide internal and exterior surface areas [32].

In the present study, leaf powder of breadfruit (*Artocarpus altilis*) leaf biochar was employed as an adsorbent to successfully remove the anionic dye Congo red (CR) dye from an aq. solution. The breadfruit biochar is being prepared at a low temperature in the air atmosphere avoiding conventional methods of biochar preparation such as high-temperature pyrolysis which takes place between 300°C and 700°C and hydrothermal carbonization between the temperatures 200°C and 350°C. The main disadvantages of the conventional method are the high-temperature burden on the environment and electricity consumption. Very few pieces of literature have reported on the preparation of biochar less than 200°C. Breadfruit is one of the rare fruits in India and is found in the Konkan range and coastal plains of Kerala. The impact of several factors such as time, dye concentration, pH, and adsorbent dose on dye removal from an aqueous solution was also examined. The response surface methodology (RSM) approach was employed to optimize the sorption process variables. Using equilibrium and kinetics, adsorption capacity and rate equation were investigated.

2. Materials and Methods

2.1. Materials. Breadfruit leaves were collected from Sulthan Bathery, India, in January and February 2022. HCl and NaOH pellets are purchased from Isochem Laboratories Angamaly, Kochi, India. Nice Chemicals (P) Ltd., Kochi, India, sold the Congo red dye that was acquired.

2.2. Preparation of Breadfruit Biochar. The leaves of breadfruit were washed and rinsed with deionized water to remove dust and soluble toxins. The leaves were kept in an oven for drying at 50°C for 24 h until their color turned yellow. Then, the leaves were crushed in a pestle and mortar and sieved with 45-mesh screens. Subsequently, 5 g of dry breadfruit leaves was added to 50 mL of 42% HCl and then stirred in the beaker. The mixture was carbonized in the hot air oven for one hour at 150°C. Then, it was filtered, dried at 90°C for 4 h, and then ground into a powder [33].

2.3. Adsorption Experiments. The parameters, initial Congo red concentration, breadfruit leaf biochar dose, pH, and time, were optimized through response surface methodology. An experimental model of the process variables was done using the Box-Behnken design (BBD). The adsorption equilibrium studies were carried out with pH 6.37, time 105 min, dye concentration of 45 mg/L, and biochar dosage in the range from 0.3 to 2 g/100 mL. The batch kinetic studies were performed in a three-neck flask and Teflon stirrer of 500 mL capacity. Different dosage amounts of 2 g and 4 g biochar were added to 450 mL of 45 mg/L of dye concentration pH 6.37. The rate of dye adsorption on biochar was evaluated by monitoring concentration over time.

Using Equations (1) and (2), we computed the dye removal and adsorption capacities [34]

$$\%\text{of dye removed}, \%R = \frac{(C_o - C_e)}{C_o} \times 100, \tag{1}$$

$$\text{adsorption capacity}, q_e = \frac{V(C_o - C_e)}{w}, \tag{2}$$

where q_e (mg/g) is the breadfruit leaf biochar capacity, w (g) is the wt. of biochar, V (L) is the vol. of Congo red sol., and C_o and C_e (mg/L) are the solutions' initial and final dye conc.

2.4. Optimization of Process Parameters. To find the optimal values for the starting dye concentration, adsorbent dose, solution pH, and temperature, this work employs a four-level Box-Behnken design (BBD) within the RSM framework. Statistical analysis software (Design-Expert software version 6.0 Stat-Ease) was used to calculate the significance of each factor, interaction, and quadratic term in the optimization process. Each variable had three distinct levels: −1, 0, and +1, representing low, medium, and high values, respectively. Table 1 depicts the arrangement of the factorial design.

The BBD method with four factors needs 29 runs, and there should be five replicates of the center points. It is possible to increase the precision of estimates of effects through the use of replication, as well as to obtain additional information on the background process variation. By including

Table 1: Levels of the four variables of adsorption process.

Description	Variable	Unit	Level		
			−1	0	1
Dye initial concentration	A	mg/L	5	27.5	50
Dosage of adsorbent	B	g/100 mL	0.5	1.25	2
pH	C	—	6	7.5	9
Time	D	min	30	135	240

center points in the analysis, it is possible to verify whether or not the predicted equations are accurate [35]. The BBD approach is used to establish quadratic regression equations (3) in terms of both the experimental data and the statistical parameters.

$$Y = \beta_O + \sum_{i=1}^{4} \beta_i X_i + \sum_{i=1}^{4} \sum_{j=1}^{4} \beta_{ij} X_i X_j + \sum_{i=1}^{4} \beta_{ii} X_i^2, \quad (3)$$

where Y is an objective to optimize the response, β_0 is the constant coefficient, β_i is the linear coefficient, β_{ii} is the quadratic coefficient, and β_{ij} is the interaction coefficient, while X_i and X_j are the coded values of the independent factors.

2.5. Characterization. The crystallographic structure of biochar can be determined using X-ray diffraction analysis (XRD), which can be conducted on a Rigaku Ultima X-ray diffractometer. FTIR identifies functional groups in biochar adsorbent and is performed in PerkinElmer (Spectrum Version 10.4.00). The surface structure and content of the biochar adsorbent were examined using Gemini 300 SEM.

3. Results and Discussion

3.1. Biochar Characterization. XRD is a method that entails irradiating a material with inbound X-rays and then measuring both their intensity and scattering angles as they depart the material. Materials are identified through XRD analysis based on their diffraction pattern. X-ray diffractometer results show that the structure of biochar is amorphous. Figure 1(a) illustrates the XRD spectrum before and after adsorption. Before adsorption shows relatively high 2-theta diffraction peaks at 22°, 26°, and 38°. After Congo red adsorption on biochar adsorbent, there was the appearance of more peaks compared to fresh biochar absorbent. Congo red adsorbed on biochar produced a new peak at 23°, 27°, and 33°.

Scherer's equation [34] was utilized to determine the differential in average size between the biochar adsorbent before and after adsorption. The average size of the biochar was determined, and it is 190.47 nm. After adsorption, the average size of the biochar increased significantly. After Congo red adsorption, the average size was 460 nm.

FTIR was used to identify and characterize unknown components, locate additives, and detect decomposition and oxidation in biochar. Before and after adsorption, band intensity and vibration shifted as a result of the change in FTIR. The presence of carbonyl (–C=O), hydroxyl alcoholic (–OH), and amino ($–NH_2$) functional groups on the biochar surfaces during the adsorption process, as well as the possibility of associations with the ($–SO_3H$) functional groups of Congo red dye molecules during the sorption process, can be seen in adsorbent spectral differences before and after adsorption [35, 36]. Table 2 gives the FTIR band adsorption frequencies before and after adsorption. The biochar reported in the intensities of the peak at 3340 cm^{-1}, 2924 cm^{-1}, and 1625 cm^{-1} reveals unbound –OH, aliphatic C–H group, and C=O group as reported similar by acid-modified pine cone powder [37].

The region under 1000 cm^{-1} implies the complex interacting vibration and represents no functional group (fingerprint region) [38]. Peaks at 1625 cm^{-1} and 1545 cm^{-1} are characteristic of red azo dyes [39]. The band at 3454 cm^{-1} represents hydroxyl (–O–H) stretching vibration of lignin, cellulose, and hemicelluloses [40], and the short band around 2946 cm^{-1} is associated with (–C–H) stretching [41, 42], and the bands at 1623 cm^{-1} and 1542 cm^{-1} reflect stretching vibrations of –C=O of esters and acids [43] and aliphatic (–C–O) stretching [44, 45], respectively. The FTIR analysis of breadfruit leaf biochar adsorbent before and after adsorption of Congo red dye is shown in Figure 1(b).

FESEM–EDX (field emission scanning electron microscopy with energy-dispersive X-ray spectroscopy) is a strong device for evaluating objects' morphology and elemental composition [46]. An SEM image (Figures 1(c) and 1(d)) clearly shows the lumpy and porous surface morphology. The average size of the breadfruit biochar was determined and was 145 nm. The dye molecules filled the pores of the biochar after being adsorbent to Congo red, demonstrating the adhesion on the surface of the adsorbent. The existence of a large volume of pores suggests that the biochar has a significant availability of dye for adsorption and trapping. High temperatures cause the breakdown of lignocellulosic material, followed by the evaporation of volatile substances, resulting in a significant pore structure forming on the surface of the adsorbents, resulting in samples with well-developed pores. These pores allowed a reasonable surface area for Congo red dye to be trapped and absorbed into the biochar [47]. Sarkar et al. [48] reported similar SEM analysis results in preparing adsorbent from rice husk ash. From Figures 1(e) and 1(f), EDX spectra, the carbon content of the biochar was found to have risen when the adsorbent was activated [49, 50].

3.2. Optimization of Sorption Variable RSM-BBD. The modeling was carried out by adjusting the first- or second-order polynomial equation to the experimental results of the response. Analysis of variance (ANOVA) was performed

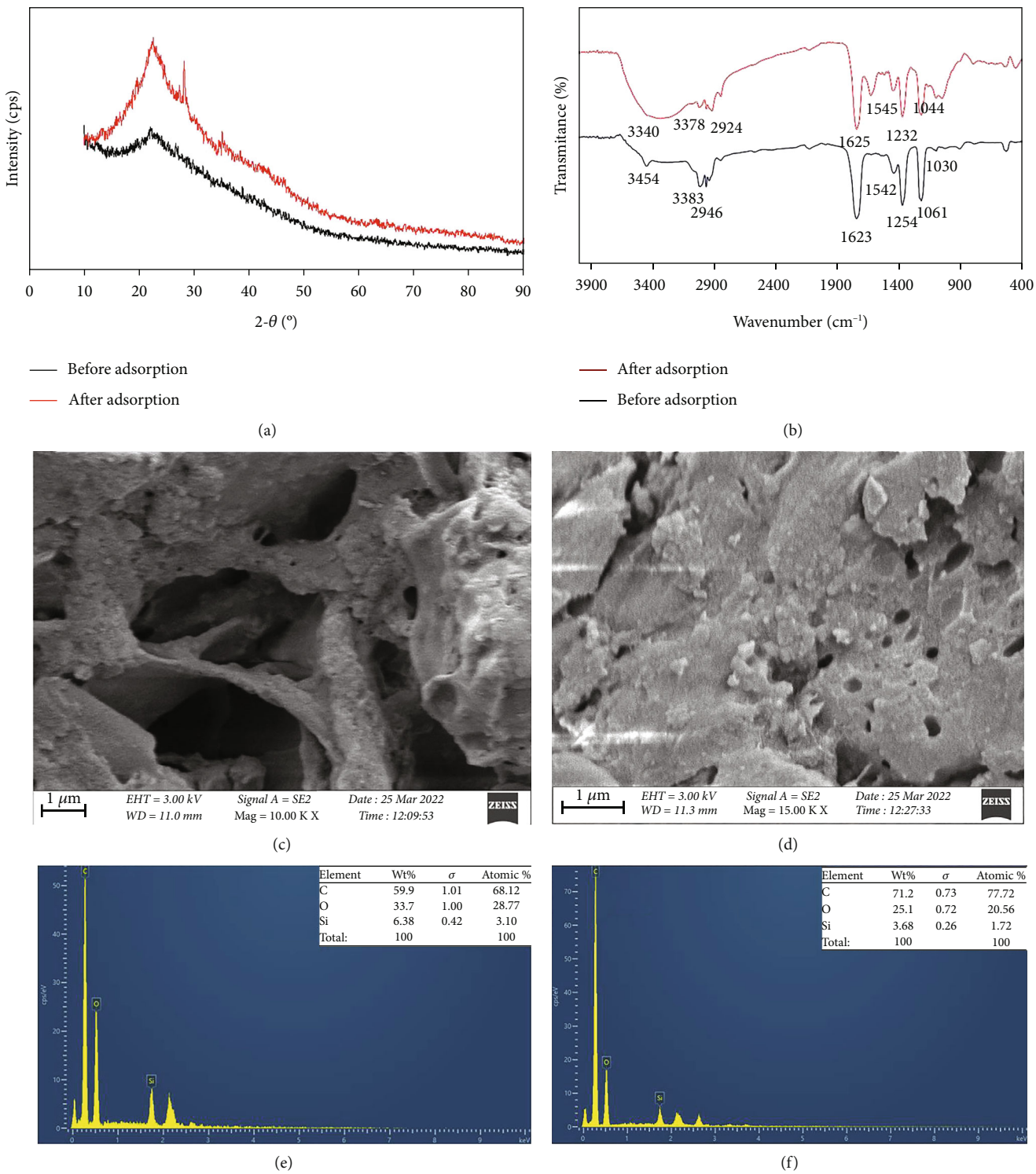

FIGURE 1: Breadfruit leaf biochar characterization: (a) XRD analysis, (b) FTIR analysis, (c, d) SEM images, and (e, f) EDX spectra of before and after adsorption of Congo red dye, respectively.

to confirm the adequacy of the predicted model by assessing the lack of fit, regression coefficient (R^2), and Fisher test value (F value). The validated model can be plotted in the form of a 3D graph to generate surface response for the determination of the best operation conditions.

The effect of operational parameters such as concentration, dosage pH, and time on the adsorption capacity of biochar for the removal of Congo red was investigated using the Box-Behnken design (BBD). The Box-Behnken design (BBD) was used to optimize the parameters and suggest

Table 2: FTIR band absorption frequencies of breadfruit leaf biochar adsorbent before and after adsorption of Congo red dye.

Sl. no.	FTIR spectra cm^{-1}	Before adsorption	After adsorption
1	-O-H	3454 (alcohol)	3340 (acids)
2	-N-H	3383	3378
3	-CH	2946	2924
4	-C=O	1623	1625
5	-C-O	1542	1545
6	$-SO_3$	1254	1232
7	-C-N	1061	1044
8	-N=N	1030	—

viable models with fewer experimental runs, hence reducing both the labor and operational costs. Equation (4) is the empirical model describing the relationship between adsorption efficiency and independent variables.

$$\begin{aligned} R(\%) = {} & -17.78963A + 9.15344B + 13.42143C + 0.19569D \\ & - 0.13007AB - 0.098444AC - 0.000994709AD \\ & - 0.74444BC - 0.00812698BD - 0.016714CD \\ & - 0.014739A^2 + 0.99674B^2 - 0.3897C^2 \\ & - 0.0000618443D^2, \end{aligned} \tag{4}$$

where R is the removal efficacy, A is the dye solution conc., B is the amount of biochar (g/100 mL), C is the pH, and D is the time.

Table 3 shows the observed and predicted Congo red dye removal efficiency, whereas the analysis of variance (ANOVA) for Congo red dye sorption is given in Table 4.

F value and p value revealed quadratic model significance. Model terms are significant if p values (prob > F) are less than 0.05 [34]. The model's F value of 33.24 suggests that it is statistically significant. Table 5 shows the standard fit statistics. The R^2 (0.97) and adjusted R^2 (0.94) difference is 0.2, indicating that the RSM model produced is connected to tangible outcomes [51].

Table 6 summarizes and shows the findings of the lack-of-fit (LOF) tests. LOF is a diagnostic method for model suitability that analyzes the pure error, which relied on duplicate measurements, to the LOF, which is based on model performance and is used to determine if a model is adequate [52, 53]. When the p value was more than 0.05, it was determined that the LOF was not statistically significant [34]. Accordingly, the LOF was not statistically significant in this case, since the p value was 0.151.

The "lack-of-fit F value" of 1.6 reflects that the LOF is significant, which is associated with a pure error [54]. According to the adsorption process, the sum of square values represents the relevance of the specified factors [35, 55].

Figure 2(a) shows the predicted vs. actual Congo red removal efficiency graph. The values for both cases are clustered around a straight line, as shown by the graph (Figure 2(a)), which also shows that the actual values and the predicted values are very close to one another and that the experimental responses and the statistically predicted responses are unambiguously correlated [34, 56, 57].

If the data are not normally distributed, the typical Box-Cox plot (Figure 2(b)) is employed to verify their normal distribution and calculate the power transformation amount needed to be integrated into the response data [34]. The Box-Cox plot in Figure 2(b) for the Congo red removal reported that the best λ is 1. The high value of the confidence interval (CI) is 3, while the low value is −2.8. The best λ is 1, which falls between the extremes of CI value indicating that no transformation power is advised. The perturbation and desirability plots shown in Figure 2(c) show the effect of all parameters employed in this study at the design space's center point [58]. The perturbation plot is useful for comparing all of a variable's effects at a single place in the design space. Over the response range, only one variable changes while all other parameters remain constant.

3.3. Influence of Parameters on Sorption. The impact of each of the factors on the dye sorption process is depicted using a three-dimensional (3D) plot. The curvatures of the plots show the interaction between the factors [59]. The 3D plots were drawn between the amount of biochar dose and initial concentration of the dye, pH, and time to analyze their interaction. The created model's 3D response surface curves shown in Figure 3 depict the mutual interactions of the chosen adsorption process parameters.

3.3.1. Influence of Dosage of Adsorbent. We examined the influences of breadfruit leaf biochar dosage on Congo red dye removal from 0.5 to 2 g/100 mL Congo red solution. From Figures 3(a), 3(b, ii), and 3(c, ii), when the amount of biochar that is being utilized for the removal of Congo red is increased, the adsorption also rises [58]. More than 99% of Congo red adsorption took place during the 105 min and reached equilibrium. The optimum dosage given by the model is 1.92 g/100 mL, and equilibrium had been reached at this point. This stage also reflects each adsorbent's maximal adsorption capacity under specific operating conditions [59]. More adsorption sites are available due to the increased surface area of biochar pores and the higher dose of biochar, which increases adsorption.

3.3.2. Influence of pH. The color of the Congo red solution shifts from red to dark blue when the pH value of the solution drops. The degree and kind of ionic character of the Congo red molecules depend on the pH of the medium [34], as can be seen by the color fluctuations with pH. At pH values in the range from 6 to 9, the effect of the dye solution and initial pH on the sorption capacity of breadfruit biochar at Congo red equilibrium was investigated. Figure 3(b) (i and ii) shows the efficiency of biochar for the removal of dyes along with the initial pH of the solution. The maximum removal efficiency (99.96%) for Congo red was observed at pH 6.37. Likewise, Congo red sorption on Macauba cake and Macauba cake thermally treated was good at pH 6.5 than at pH 10 [60]. Dye adsorption increases when the pH is between 6 and 7 and then decreases as the

Table 3: Box-Behnken design (BBD) for adsorption of Congo red dye on breadfruit leaf biochar adsorbent.

Run	*A*: concentration (mg/L)	*B*: dosage of adsorbent (g/100 mL)	*C*: pH	*D*: time (min)	Actual removal efficacy (%)	Predicted removal efficacy (%)
1	5	0.5	7.5	135	76.9	77.18
2	50	0.5	7.5	135	98.92	99.99
3	5	2	7.5	135	86.09	83.65
4	50	2	7.5	135	99.33	99.06
5	27.5	1.25	6	30	87.41	88.81
6	27.5	1.25	9	30	98.59	99.12
7	27.5	1.25	6	240	97.98	97.46
8	27.5	1.25	9	240	98.63	97.24
9	5	1.25	7.5	30	75.48	75.13
10	50	1.25	7.5	30	99.86	99.62
11	5	1.25	7.5	240	84.26	83.21
12	50	1.25	7.5	240	99.24	98.31
13	27.5	0.5	6	135	94.45	92.49
14	27.5	2	6	135	97.8	96.25
15	27.5	0.5	9	135	98.95	99.21
16	27.5	2	9	135	98.95	99.62
17	5	1.25	6	135	70.67	73.13
18	50	1.25	6	135	99.4	99.57
19	5	1.25	9	135	83.71	84.82
20	50	1.25	9	135	99.15	97.97
21	27.5	0.5	7.5	30	95.54	93.72
22	27.5	2	7.5	30	96.59	97.08
23	27.5	0.5	7.5	240	97.59	98.38
24	27.5	2	7.5	240	96.08	99.18
25	27.5	1.25	7.5	135	97.45	97.21
26	27.5	1.25	7.5	135	97.56	97.21
27	27.5	1.25	7.5	135	95	97.21
28	27.5	1.25	7.5	135	98.1	97.21
29	27.5	1.25	7.5	135	97.95	97.21

pH increases. Furthermore, as the initial concentration was increased, the adsorption yields gradually increased. The maximum sorption efficiency was 99.96% at a low initial dye concentration (27.5 mg/L) and a pH of 6.37. The experiment showed that the percentage of adsorption falls as the pH of the dye solution raises. The sorption of an anionic dye reduces when pH rises, and this phenomenon is linked to both the negative charge on the surface of the biochar and the presence of excess OH ions in the solution, which compete for sorption sites [61]. The pHzpc value for breadfruit biochar was found to be 6.8 (Figure 4) which is more than the pH at which the removal efficiency is maximum. When $pH < pHzpc$, the surface of the biochar would get protonated and creates a competition of dye molecules for the available sites.

3.3.3. Influence of Initial Congo Red Concentration. To investigate the influence that dye concentration has on Congo red dye removal, the initial concentrations of the dye solution were varied throughout a wide range, from 5 to 50 mg/L. Figure 3(a) illustrates the influence of biochar and Congo red concentration on Congo red removal from biochar. At higher concentrations of dye solution, the adsorption was unaffected. Because many dye molecules occupy the adsorbent surface [33], the equilibrium (q_e) rises with increasing dye concentration, resulting in more significant adsorption at high concentrations [62]. At a concentration of 45 mg/L, Congo red reached its maximal molecular occupancy. An increase in Congo red concentration had no noticeable effect on the amount of dye that was adsorbed. As a direct consequence of this, the initial dye concentration has the greatest impact on Congo red adsorption.

3.3.4. Influence of Time. The role of time in dye adsorption was examined by doing trials from 30 min to 240 min. The removal rate increased with the initial Congo red concentration; the removal rate (percent) increased as the reaction time increased. Figure 3(c) (i and ii) shows the combined effect of the biochar and the concentration of Congo red on removal at varying time intervals (30–240 min). The findings revealed that the adsorption of dye started rising with an increase in time and effectiveness up to 105 min and that,

Table 4: Response surface quadratic model for adsorption of Congo red dye on breadfruit leaf biochar adsorbent: ANOVA results.

Source	Sum of squares	df	Mean square	F value	p value prob > F	
Model	1806.05	14	129	33.24	<0.0001	Significant
A: concentration	1175.92	1	1175.92	302.95	<0.0001	
B: dosage of adsorbent	13	1	13	3.35	0.0886	
C: pH	76.36	1	76.36	19.67	0.0006	
D: time	34.37	1	34.37	8.86	0.01	
AB	19.27	1	19.27	4.97	0.0428	
AC	44.16	1	44.16	11.38	0.0046	
AD	22.09	1	22.09	5.69	0.0317	
BC	2.81	1	2.81	0.72	0.4095	
BD	1.64	1	1.64	0.42	0.5264	
CD	27.72	1	27.72	7.14	0.0182	
A^2	361.16	1	361.16	93.05	<0.0001	
B^2	2.04	1	2.04	0.53	0.4805	
C^2	4.99	1	4.99	1.28	0.276	
D^2	3.02	1	3.02	0.78	0.393	
Residual	54.34	14	3.88			
Lack of fit	47.94	10	4.79	2.99	0.151	Not significant
Pure error	6.4	4	1.6			
Cor. total	1860.39	28				

Table 5: Quadratic model for adsorption of Congo red dye on breadfruit leaf biochar adsorbent: standard fit statistics.

Std. dev.	1.97
Mean	93.71
C.V. %	2.1
PRESS	286.13
R^2	0.9708
Adj. R^2	0.9416
Pred. R^2	0.8462
Adeq. precision	19.927

after 105 min, no significant adsorption was observed, and removal efficiency decreased. Large biochar surface area increased the initial adsorption rate. Because there were a significant number of easily accessible active places on the biochar surface, the process started quite quickly. However, as time went on, the active sites were occupied by Congo red molecules, which slowed down the process until it finally reached a saturated state [15, 63].

3.4. Model Confirmation and Validation. An optimization technique called RSM-BBD was used with four variable interactions carried out under various factors to optimize all the responses and runs. The initial dye concentration (5–50 mg/L), biochar dose (0.5–2 g), pH (6–9), and time (30–240 min) were all chosen to maximize dye removal efficiency. Under optimal conditions, with an initial Congo red concentration of 45 mg/L, an amount of biochar of 1.98 g/100 mL, a pH of 6.37, and a contact time of 105 min, the dye removal efficiency was 99.96%.

3.5. Equilibrium Studies on Breadfruit Biochar. Adsorption characteristics and equilibrium parameters give the nature of the biochar-Congo red interaction. The equilibrium data are correlated using Freundlich, Langmuir, and Dubinin–Radushkevich isotherms [64] in this work. These models were utilized to analyze experimental sorption equilibrium parameters to learn more about the surface characteristics of the biochar and its affinity for the Congo red dye.

Langmuir isotherm model

$$\frac{1}{q_e} = \frac{1}{K_L q_m C_e} + \frac{1}{q_m}. \tag{5}$$

Freundlich isotherm

$$\ln(q_e) = \frac{1}{n} \ln(C_e) + \ln(K_F). \tag{6}$$

q_e is the Congo red adsorbed by biochar at equilibrium (mg/g), C_e is the equilibrium concentration of biochar (mg/L), q_m is the biochar sorption efficiency (mg/g), and K_L is the Langmuir constant (L/mg). n and K_F (mg/g) are Freundlich isotherm constants.

To identify between physical and chemical adsorption, the Dubinin–Radushkevich (DR) isotherm is used. It is represented by [64]

$$q_e = q_D \exp\left(B_D \varepsilon_d^2\right), \tag{7}$$

Table 6: Quadratic model for adsorption of Congo red dye on breadfruit leaf biochar adsorbent: lack-of-fit statistics.

Source	Sum of squares	Mean df	F Square	p value	prob > F	
Linear	554.34	20	27.72	17.31	0.0067	
2FI	436.65	14	31.19	19.48	0.0055	
Quadratic	47.94	10	4.79	2.99	0.151	Suggested
Cubic	6.58	2	3.29	2.05	0.2433	Aliased
Pure error	6.4	4	1.6			

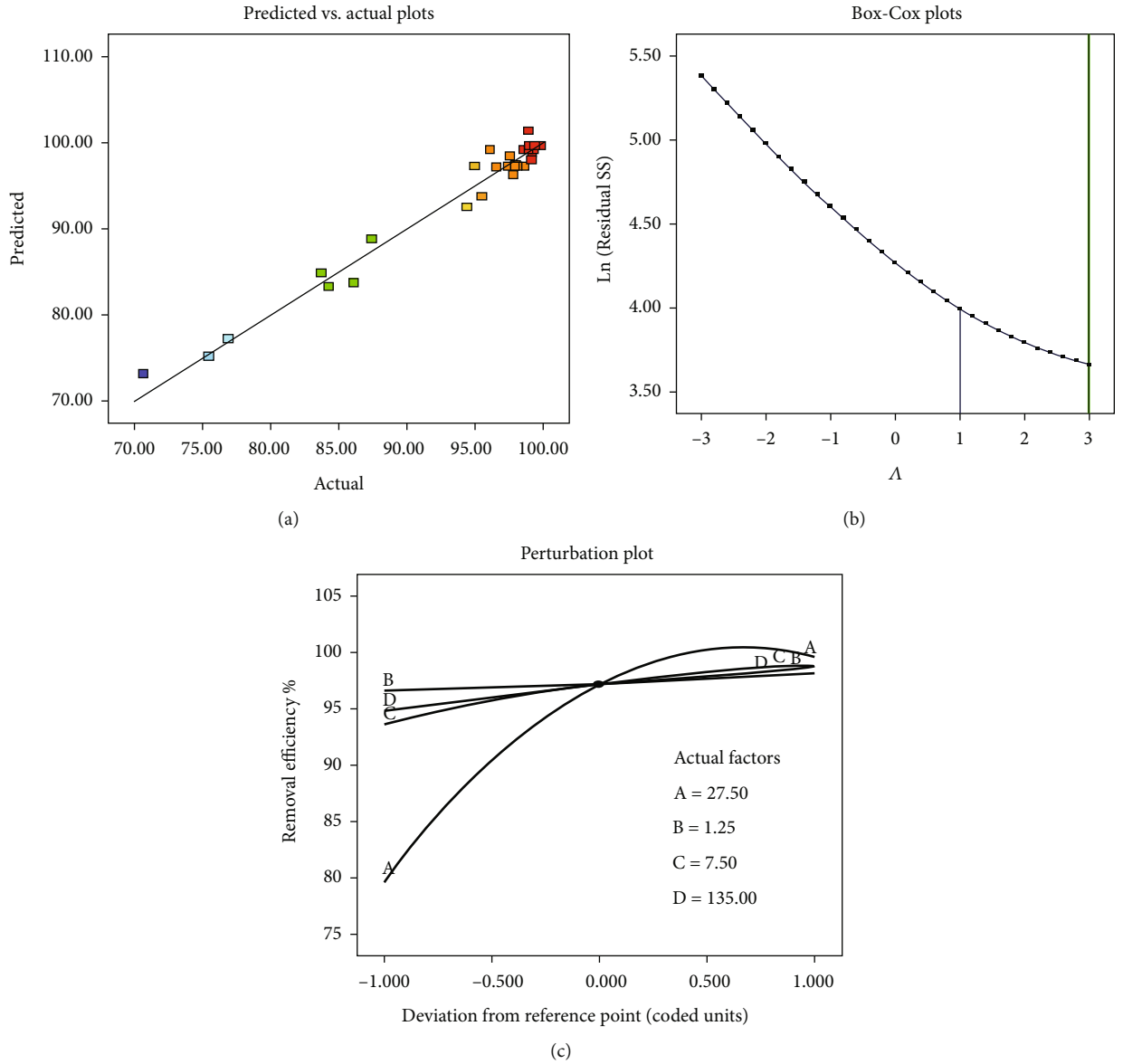

Figure 2: (a) Predicted vs. actual plots; (b) Box-Cox plots; (c) perturbation plot for adsorption of Congo red dye on breadfruit leaf biochar adsorbent.

where q_D is the DR isotherm constant (mg/g), ε_d is the Polanyi potential (kJ/mol) related to C_e is given in

$$\varepsilon_d = RT \ln\left(1 + \frac{1}{C_e}\right), \tag{8}$$

where R refers to the gas constant and T refers to the temperature (K). The value B_D (mol^2/kJ^2) and the mean free energy of sorption E (kJ/mol) are connected with

$$E = \frac{1}{\sqrt{2B_D}}. \tag{9}$$

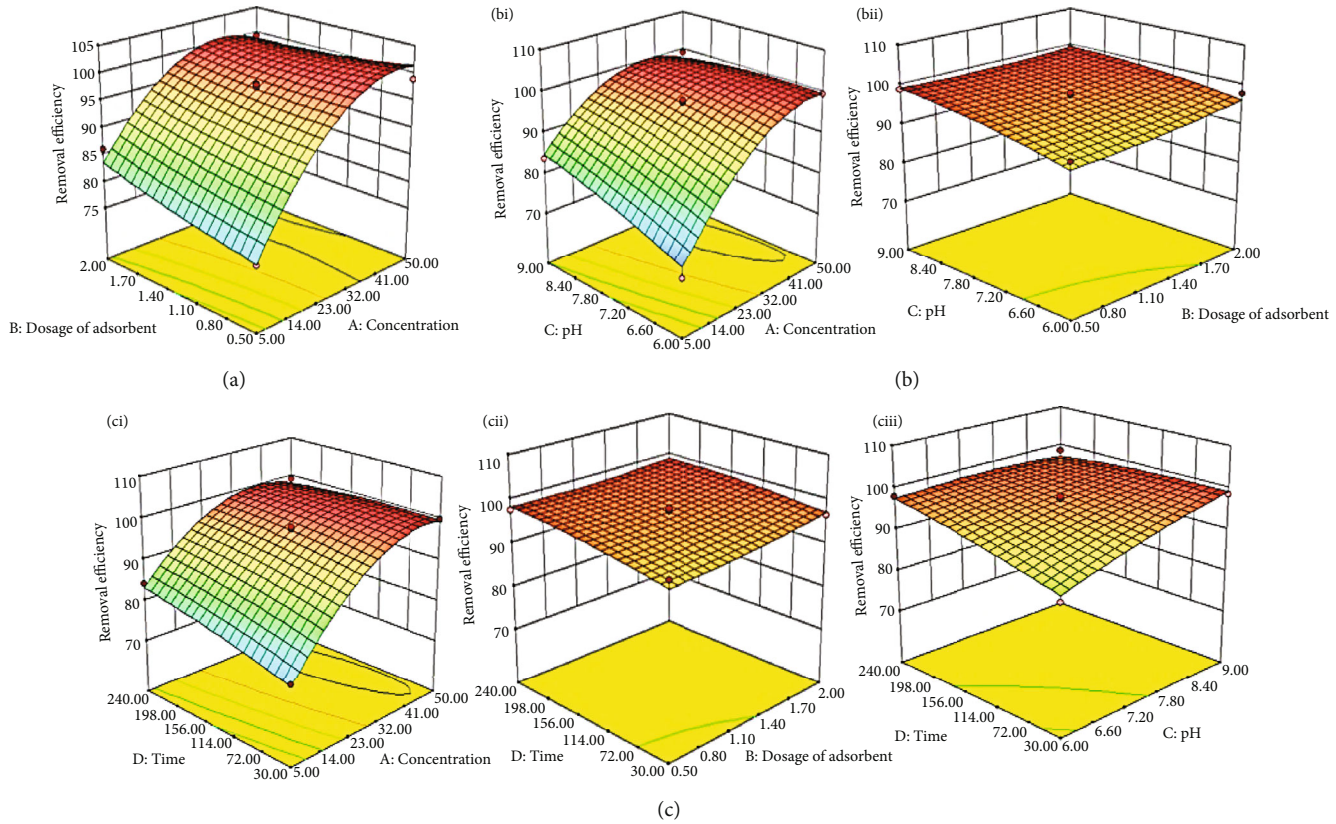

FIGURE 3: 3D surface plots comparing the percentage of Congo red removed with breadfruit leaf biochar vs. (a) concentration and dosage of biochar, (b, i) concentration and pH, (b, ii) pH and dosage of biochar, (c, i) time and concentration, (c, ii) time and dosage of biochar, and (c, iii) time and pH.

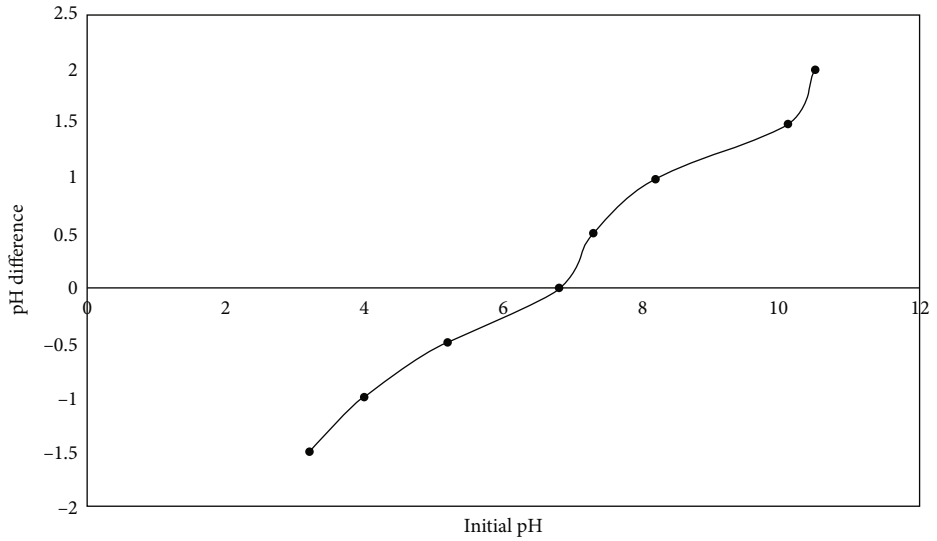

FIGURE 4: The graph determining pHzpc of breadfruit leaf biochar adsorbent.

The parameters of the equilibrium model that were computed are shown in Table 6 and represented in Figure 5. From Table 7, it was observed that the equilibrium data follows the Langmuir isotherm because the R^2 value is 0.98 when compared to the other two models. It is assumed that Congo red adsorption onto charcoal results in monolayer coverage on roughly homogenous binding sites, which is supported by the Langmuir model [65]. According to the findings of the DR model, the value of E is less than 8 kJ/mol, suggesting that the adsorption is a physical adsorption process. Similar experiments, such as the equilibrium results for Congo red adsorption on jute stick powder, demonstrate

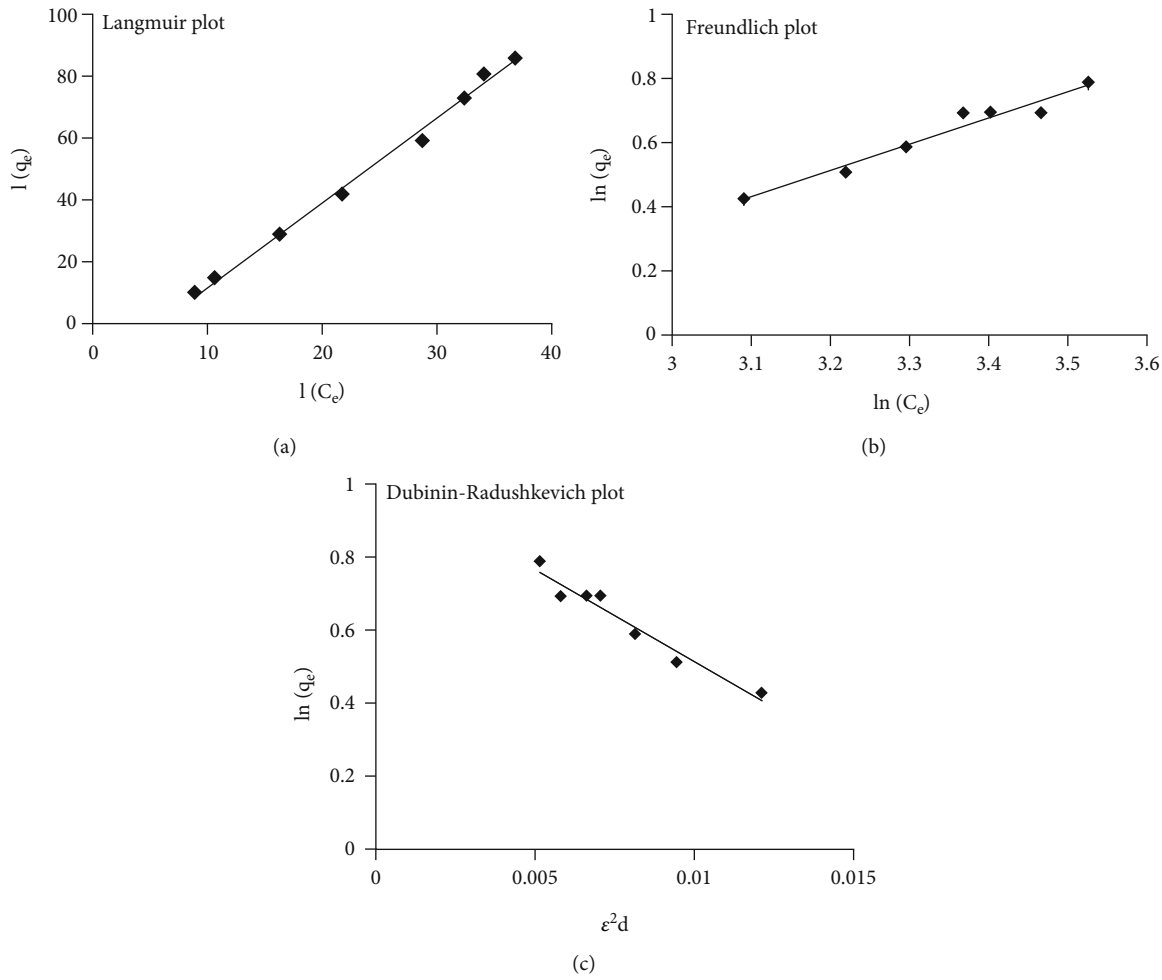

Figure 5: Equilibrium model plots of biochar-Congo red dye adsorption system: (a) Langmuir plot; (b) Freundlich plot; (c) Dubinin–Radushkevich plot.

Table 7: Calculated various equilibrium model parameters for adsorption of Congo red dye on breadfruit leaf biochar adsorbent.

Langmuir			Freundlich			Dubinin–Radushkevich			
q_m (mg/g)	K_L (L/mg)	R^2	K_F (mg/g)	n	R^2	q_D (mg/g)	B_D (mol^2/kJ^2)	E (kJ/mol)	R^2
17.81	0.004	0.98	0.12	1.217	0.95	2.78	50.89	0.0991	0.9491

a good concordance with the Langmuir model, with $R^2 = 0.999$ [66]. Congo red removal from wastewater was investigated using cattail root fitted into the Langmuir model, and the results were promising [67]. The adsorption of Congo red on breadfruit biochar is compared to that of other biosorbents in Table 8.

3.6. Kinetics of Breadfruit Biochar. Different samples of the biochar–Congo red solution were taken at varying time intervals, and the concentration of the solution was evaluated to study the adsorption kinetics. To figure out how Congo dye adsorbs on biochar, three kinetic models were used: pseudo-first-order [76, 77], pseudo-second-order [77, 78], and Elovich kinetic model [79], and the intraparticle diffusion kinetic equation [80].

The pseudo-first-order (PFO) model is given in equation nonlinear (10) and linear (11) forms:

$$q_t = q_e\left(1 - e^{k_f t}\right), \tag{10}$$

$$\ln\left(q_e - q_t\right) = \ln\left(q_e\right) - k_f t. \tag{11}$$

The pseudo-second-order (PSO) model is given in equation nonlinear (12) and linear (13) forms:

$$q_t = \frac{k_s q_e^2 t}{1 + k_s q_e t}, \tag{12}$$

Table 8: Comparison of adsorption capacity of breadfruit leaf biochar with other biochar adsorbents for Congo red dye adsorption.

S. no.	Name of the adsorbent	Adsorption capacity, q_m (mg/g)	Reference
1	Water hyacinth roots	13.46	[68]
2	Punica granatum (pomegranate rind) activated carbon	100	[69]
3	Indian Jujuba seeds	55.56	[70]
4	Banana peels	18.2	[71]
5	Phoenix dactylifera leaves	25.31	[72]
6	Wet-torrefied microalga	164.35	[73]
7	Cotton stalks	250.0	[74]
8	Green pea peels	62.11	[75]
9	Breadfruit	17.81	Present study

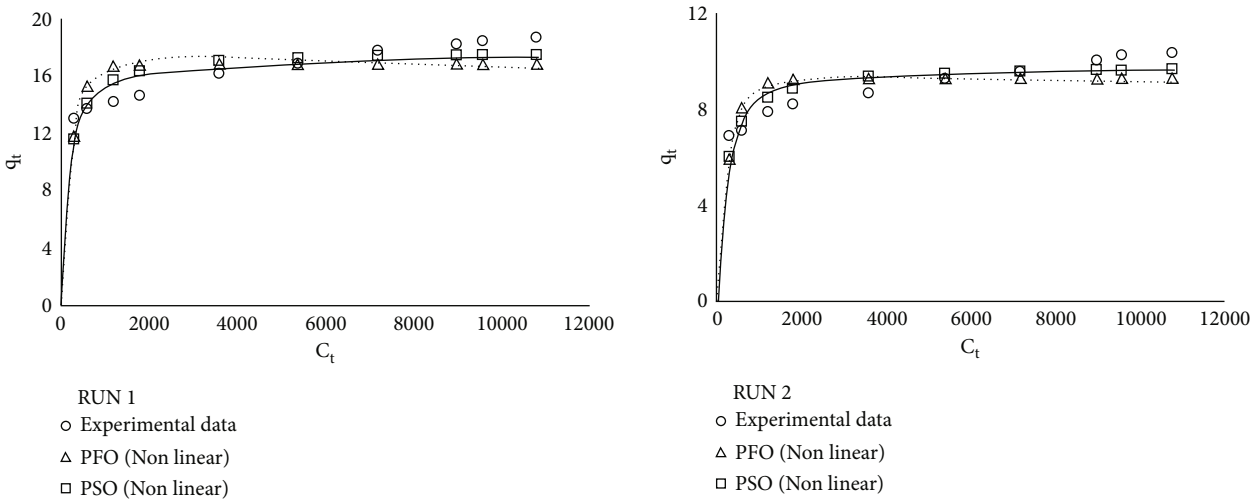

Figure 6: Nonlinear plots of PFO and PSO kinetic models for the adsorption of Congo red dye on breadfruit leaf biochar.

$$\frac{1}{q_t} = \frac{1}{k_s q_e^2} + \frac{t}{q_e}. \tag{13}$$

The Elovich kinetic model is given in

$$q_t = \frac{1}{\omega} \ln(\alpha\omega) + \frac{1}{\omega} \ln(t). \tag{14}$$

The intraparticle diffusion model (IPD) is given in

$$q_t = k_d t^{1/2} + I, \tag{15}$$

where q_t is the sorption capacity at time t (mg/g), k_f is the rate constant for PFO (1/s), k_s is the rate constant for PSO (g/mg s), $\propto$ is the rate of adsorption initially, β is the rate of adsorption at time t, k_d is the IPD rate (mg/g $s^{1/2}$), and I is the adsorption boundary layer thickness.

The nonlinear forms of the PFO and PSO kinetic models for the adsorption of Congo red ions on breadfruit leaf char husk are presented in Figure 6 by plotting q_t vs. t, and the measured constants and theoretically derived q_e are given in Table 9. The linearized expression for the PFO and PSO kinetic models is given in Figures 7(a) and 7(b), and the derived parameters from the slope and intercept are reported in Table 9. The coefficient of determination R^2 was utilized as a deciding tool for the best-fit kinetic equations to determine the applicability of different models. Table 9 displays the computed R^2 values for linear and nonlinear equations. The estimated values of R^2 for nonlinear models of PFO are 0.97 and 0.95 and those of PSO were 0.99 and 0.99, for runs 1 and 2, respectively, indicating that the PSO model appears to be more convincing for calculating kinetic parameters for Congo red adsorption on breadfruit leaves.

The computed rate constant values for linear and nonlinear variants of PSO (Table 9) were quite similar. The difference in the values generated by different linearized models utilizing the same experimental data might be attributed to the degree of difficulties and challenges involved with the linearization of a nonlinear form [81, 82]. Given these characteristics, it is preferable to use a nonlinear formula to calculate the kinetic parameters since the error distribution does not change throughout execution [82]. The PSO rate constant, k_s, indicates that sorption is progressing rapidly [83]. The ionic interaction intensity in biochar and Congo red dye is high, according to the PSO model's fitness [84]. Studies of CR

Table 9: Kinetic model parameters for the adsorption of Congo red dye on breadfruit leaves biochar.

Name of the model	Run 1 (2 g)				Run 2 (4 g)			
	q_e (exp)	k_f	q_e (cal)	R^2	q_e (exp)	k_f	q_e (cal)	R^2
PFO (linear)	18.67	0.018	6.89	0.96	10.35	0.017	4.15	0.90
PFO (nonlinear)	18.67	0.004	16.82	0.97	10.35	0.003	9.267	0.95
		k_s	q_e (cal)	R^2		k_s	q_e (cal)	R^2
PSO (linear)	18.67	0.0001	19.04	0.99	10.35	0.0002	10.52	0.99
PSO (nonlinear)	18.67	0.0003	17.74	0.99	10.35	0.0005	9.801	0.99
Elovich		ω	$\alpha \times 10^{-5}$	R^2		ω	$\alpha \times 10^{-5}$	R^2
		0.605	10.01	0.95		1.006	2.37	0.96
		I	k_d	R^2		I	k_d	R^2
IPD		11.98	0.06	0.99		6.31	0.03	0.98

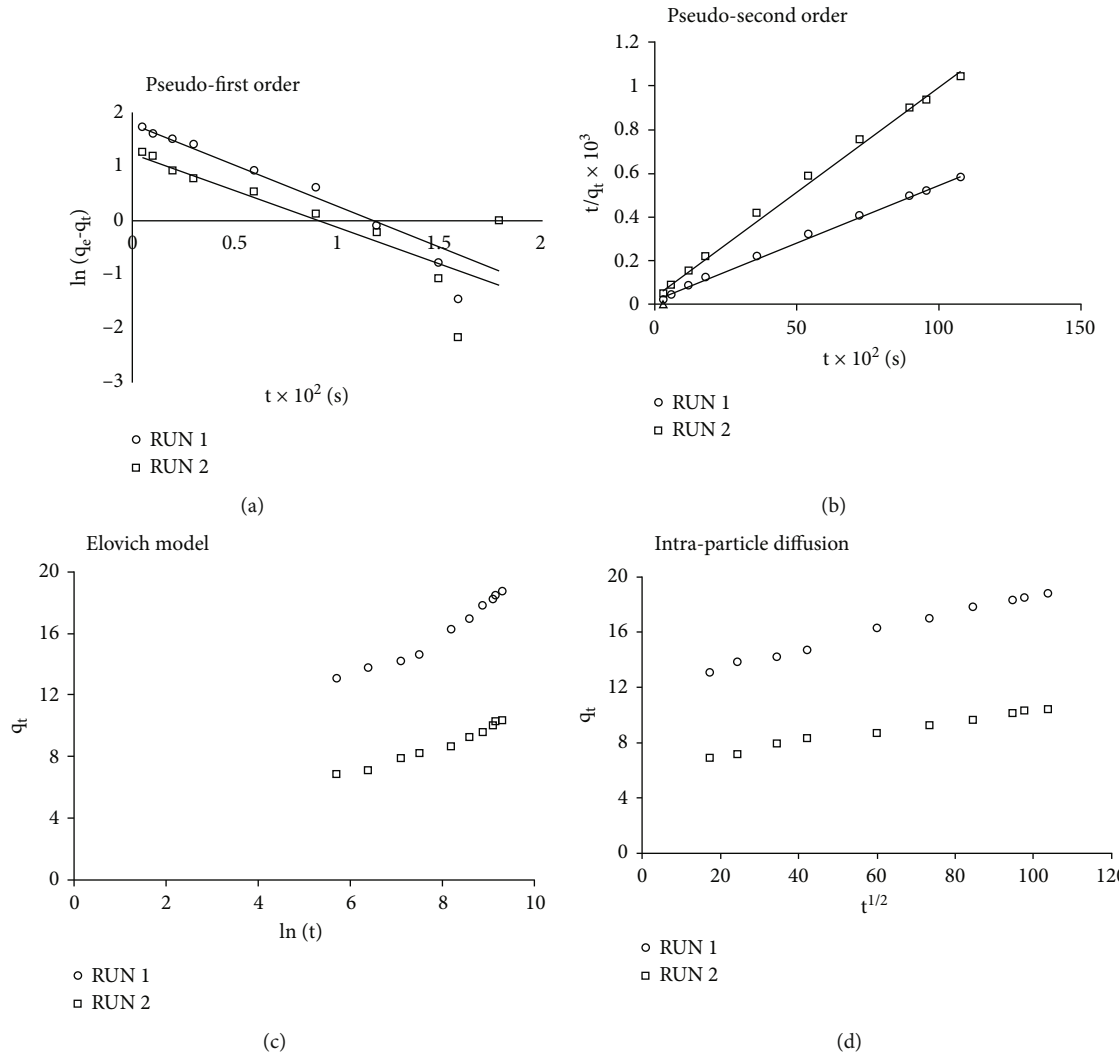

Figure 7: Linear plots of kinetic models for the adsorption of Congo red dye on breadfruit leaf biochar: (a) pseudo-first-order (PFO), (b) pseudo-second-order (PSO), (c) Elovich model, and (d) intraparticle diffusion.

adsorption behavior on banana peels [71], coir pith-activated carbon [85], and guava (*Psidium guajava*) leaf powder [86] all produced similar study results.

The kinetic data correlated with the Elovich model, and parameters were determined using a linear plot drawn between q_t vs. ln (t), shown in Figure 7(c) and are given in

Table 9. The values of R^2 are very small; therefore, this model does not describe our system.

The results on the kinetics of dye adsorption were also evaluated with the use of the IPD kinetic equation. The steps controlling the possibilities of intraparticle diffusion during Congo red molecule adsorption are the shape and size of molecules, as well as the pore size and pore size distribution of biochar [36, 87]. There are several adsorption stages, including external surface or film diffusion, pore diffusion, surface diffusion, and/or a combination of one or more processes, such as pore surface adsorption [34]. The intercept depicts the impact of the boundary layer. If the intraparticle is the only rate-determining step, the graph between q_t and $t^{1/2}$ must be linear. If not, intraparticle diffusion does not represent the sole mechanism determining rate [88–90]. Surface diffusion is represented by the first segment of the curve, whereas intraparticle diffusion is represented by the linear component [91, 92]. The intraparticle diffusion model is depicted in Figure 7(d).

3.7. Adsorption Mechanism. The present study gives the value of mean free energy of sorption as 0.099 ($<8\,\mathrm{kJ\,mol^{-1}}$), showing that the sorption is physisorption, according to the Dubinin–Radushkevich isotherm. Physisorption is caused by attractive forces of molecules such as H_2 donor-acceptor interactions and van der Waals dispersion forces [93]. Dipole-dipole interactions between both the hydrogen surface of the hydroxyl groups on the biochar and the aromatic rings in Congo red dye occur in the biochar-Congo red system, as do interactions connecting the hydrogen surface of the hydroxyl groups on the biochar and the atoms (oxygen and nitrogen; H-acceptor) of Congo red dye [94]. As previously stated, the removal of Congo by breadfruit leaf biochar supported the Langmuir equilibrium model. This isotherm is assumed to have resulted from the adsorption of adsorbate onto a microporous adsorbent (breadfruit leaf biochar), whose surface was coated in a monolayer of adsorbate (Congo red) [90]. Figure 1(b) depicts the FTIR spectrum of Congo red, and the peak at $3731\,\mathrm{cm^{-1}}$ reveals the presence of hydroxyl (OH) and NH_2 groups in the compound. The peaks at 1545, 1443, and $1368\,\mathrm{cm^{-1}}$, respectively, were caused by the amine group, –N–H bending, and –S=O stretching vibrations [58]. These biochar peaks provide strong evidence supporting the hypothesis that the mechanism of dye removal needs a simultaneous combination of adsorption and reduction [58]. Adsorption is often controlled by internal, external, or both types of mass transfer. The reluctance of the plot of q_t vs. $t^{1/2}$ (Figure 7(d)) to pass through the origin and the value of $I > 0$ (Table 9) suggested that more mechanisms are operating in the adsorption process in addition to intraparticle diffusion. The graph's biphasic character indicated that the Congo red dye adsorption process involves either film or pore diffusion [89]. In aqueous solutions, dye ions have the propensity to form their associations [38]. Self-dissociation is analogous to polymerization, which occurs when dye molecules get complex. The optimal pH for removal, according to RSM-BBD, is 6.37. Congo red is a big molecule that is negatively charged across the majority of its pH range (>5) [95]. The adsorption of anionic dyes reduces as the pH of a solution rises. As a result of the biochar surface's negative charge and the existence of excess, this is the case that the solution's OH- ions are in a contest for adsorption sites [60].

4. Conclusions

The current study examines the efficiency of biochar made from breadfruit leaves to adsorb Congo red from an aqueous solution. To identify the composition of the synthesized biochar, it was subjected to XRD, FTIR, and SEM-EDX analysis. Furthermore, the effect of time, Congo red dye concentration, pH, and breadfruit biochar dosage on dye removal from an aqueous solution was investigated and optimized using the response surface methodology. The adsorption capacity and rate equation were calculated using equilibrium and kinetic investigations. X-ray diffractometer results show that the structure of biochar is amorphous. Biochar's SEM figure illustrates an uneven, porous surface with an average size of 145 nm. According to the findings of the RSM-BBD design, breadfruit leaf biochar had a maximum adsorption efficiency of 99.96% for Congo red at a pH of 6.37, a dye concentration of 45 mg/L, a time of 105 min, and a dose of 1.92 g/100 mL, respectively. The Langmuir model matched the dye adsorption by breadfruit biochar adsorbent, which had the highest sorption capacity of 17.81 mg/g. The PSO describes the kinetics, implying homogenous, monolayer, and physicochemical adsorption.

Data Availability

The data is available in the manuscript.

Conflicts of Interest

The authors declare that they have no conflict of interest.

Authors' Contributions

Laxmi Deepak Bhatlu M. was responsible for conceptualization, methodology, and supervision; Athira P.S. was responsible for experimentation, data arrangement, validation, writing, and original draft preparation; Neethu Jayan was responsible for editing and reviewing; Debabrata Barik was responsible for supervision and reviewing; Milon Selvam Dennison was responsible for data analysis, editing, and reviewing.

Acknowledgments

The authors sincerely thank the KPR Institute of Engineering and Technology, Coimbatore, India, and Karpagam Academy of Higher Education (KAHE), Coimbatore, India, for providing the research facilities to carry out this research work.

References

[1] G. Crini, "Non-conventional low-cost adsorbents for dye removal: a review," *Bioresource Technology*, vol. 97, no. 9, pp. 1061–1085, 2006.

[2] R. Sivaraj, C. Namasivayam, and K. Kadirvelu, "Orange peel as an adsorbent in the removal of acid violet 17 (acid dye) from aqueous solutions," *Waste Management*, vol. 21, no. 1, pp. 105–110, 2001.

[3] D. Landy, I. Mallard, A. Ponchel, E. Monfier, and S. Fourmentin, "Remediation technologies using cyclodextrins: an overview," *Environmental Chemistry Letters*, vol. 10, no. 3, pp. 225–237, 2012.

[4] P. J. Harvey, B. F. Campanella, P. M. Castro et al., "Phytoremediation of polyaromatic hydrocarbons, anilines and phenols," *Environmental Science and Pollution Research International*, vol. 9, no. 1, pp. 29–47, 2002.

[5] B. Volesky, "Biosorption and biosorbents," in *Biosorption of Heavy Metals*, pp. 3–5, CRC Press, Boca Raton, 1990.

[6] J. M. Jabar, Y. A. Odusote, Y. T. Ayinde, and M. Yılmaz, "African almond (*Terminalia catappa* L) leaves biochar prepared through pyrolysis using H_3PO_4 as chemical activator for sequestration of methylene blue dye," *Results in Engineering*, vol. 14, article 100385, 2022.

[7] J. M. Jabar, I. A. Owokotomo, Y. T. Ayinde, A. M. Alafabusuyi, G. O. Olagunju, and V. O. Mobolaji, "Characterization of prepared eco-friendly biochar from almond (*Terminalia catappa* L) leaf for sequestration of bromophenol blue (BPB) from aqueous solution," *Carbon Letters*, vol. 31, no. 5, pp. 1001–1014, 2021.

[8] J. M. Jabar and Y. A. Odusote, "Utilization of prepared activated biochar from water lily (Nymphaea lotus) stem for adsorption of malachite green dye from aqueous solution," *Biomass Conversion and Biorefinery*, pp. 1–12, 2021.

[9] X. Wang, Q. Xu, L. Zhang, L. Pei, H. Xue, and Z. Li, "Adsorption of methylene blue and Congo red from aqueous solution on 3D MXene/carbon foam hybrid aerogels: a study by experimental and statistical physics modeling," *Journal of Environmental Chemical Engineering*, vol. 11, no. 1, article 109206, 2023.

[10] A. Dąbrowski, "Adsorption – from theory to practice," *Advances in colloid and interface science*, vol. 93, no. 1-3, pp. 135–224, 2001.

[11] G. Crini, "Wastewater treatment by sorption," in *Sorption Process and pollution: conventional and nonconventional sorbents for pollutant removal from waste wasters*, pp. 39–78, PUFC Publication, Besancon, 2010.

[12] G. Z. Kyzas and M. Kostoglou, "Green adsorbents for wastewaters: a critical review," *Materials*, vol. 7, no. 1, pp. 333–364, 2014.

[13] A. Dbik, S. Bentahar, M. El Khomri, N. El Messaoudi, and A. Lacherai, "Adsorption of Congo red dye from aqueous solutions using tunics of the corm of the saffron," *Materials today: proceedings*, vol. 22, pp. 134–139, 2020.

[14] A. Çelekli, S. S. Birecikligil, F. Geyik, and H. Bozkurt, "Prediction of removal efficiency of Lanaset Red G on walnut husk using artificial neural network model," *Bioresource Technology*, vol. 103, no. 1, pp. 64–70, 2012.

[15] H. Y. Zhu, Y. Q. Fu, R. Jiang et al., "Adsorption removal of Congo red onto magnetic cellulose/Fe_3O_4/activated carbon composite: equilibrium, kinetic and thermodynamic studies," *Chemical Engineering Journal*, vol. 173, no. 2, pp. 494–502, 2011.

[16] R. K. Xu, S. C. Xiao, J. H. Yuan, and A. Z. Zhao, "Adsorption of methyl violet from aqueous solutions by the biochars derived from crop residues," *Bioresource Technology*, vol. 102, no. 22, pp. 10293–10298, 2011.

[17] T. Farías, L. C. De Menorval, J. Zajac, and A. Rivera, "Benzalkonium chloride and sulfamethoxazole adsorption onto natural clinoptilolite: effect of time, ionic strength, pH and temperature," *Journal of Colloid and Interface Science*, vol. 363, no. 2, pp. 465–475, 2011.

[18] Y. Feng, F. Yang, Y. Wang et al., "Basic dye adsorption onto an agro-based waste material - sesame hull (*Sesamum indicum* L.)," *Bioresource Technology*, vol. 102, no. 22, pp. 10280–10285, 2011.

[19] Y. Yang, D. Jin, G. Wang, D. Liu, X. Jia, and Y. Zhao, "Biosorption of Acid Blue 25 by unmodified and CPC-modified biomass of *Penicillium* YW01: kinetic study, equilibrium isotherm and FTIR analysis," *Colloids and Surfaces B: Biointerfaces*, vol. 88, no. 1, pp. 521–526, 2011.

[20] M. Akgul and A. Karabakan, "Promoted dye adsorption performance over desilicated natural zeolite," *Microporous and Mesoporous Materials*, vol. 145, no. 1-3, pp. 157–164, 2011.

[21] X. Y. Huang, H. T. Bu, G. B. Jiang, and M. H. Zeng, "Cross-linked succinyl chitosan as an adsorbent for the removal of methylene blue from aqueous solution," *International Journal of Biological Macromolecules*, vol. 49, no. 4, pp. 643–651, 2011.

[22] T. Kan, X. Jiang, L. Zhou et al., "Removal of methyl orange from aqueous solutions using a bentonite modified with a new Gemini surfactant," *Applied Clay Science*, vol. 54, no. 2, pp. 184–187, 2011.

[23] B. Balci, "Basic textile dye adsorption from aqueous solution and synthetic dye bath wastewater by modified *eucalyptus* barks," *Fresenius Environmental Bulletin*, vol. 25, pp. 6124–6131, 2016.

[24] A. Xue, S. Zhou, Y. Zhao, X. Lu, and P. Han, "Effective NH_2-grafting on attapulgite surfaces for adsorption of reactive dyes," *Journal of Hazardous Materials*, vol. 194, pp. 7–14, 2011.

[25] K. Elass, A. Laachach, A. Alaoui, and M. Azzi, "Removal of methyl violet from aqueous solution using a stevensite-rich clay from Morocco," *Applied Clay Science*, vol. 54, no. 1, pp. 90–96, 2011.

[26] H. Chen, J. Zhao, A. Zhong, and Y. Jin, "Removal capacity and adsorption mechanism of heat-treated palygorskite clay for methylene blue," *Chemical Engineering Journal*, vol. 174, no. 1, pp. 143–150, 2011.

[27] M. Ghaedi, H. Hossainian, M. Montazerozohori et al., "A novel acorn based adsorbent for the removal of brilliant green," *Desalination*, vol. 281, pp. 226–233, 2011.

[28] A. Y. Dursun and O. Tepe, "Removal of Chemazol Reactive Red 195 from aqueous solution by dehydrated beet pulp carbon," *Journal of Hazardous Materials*, vol. 194, pp. 303–311, 2011.

[29] J. D. da Silveira Neta, G. C. Moreira, C. J. da Silva, C. Reis, and E. L. Reis, "Use of polyurethane foams for the removal of the Direct Red 80 and Reactive Blue 21 dyes in aqueous medium," *Desalination*, vol. 2011, no. 281, pp. 55–60, 2011.

[30] J. M. Jabar and Y. A. Odusote, "Removal of cibacron blue 3G-A (CB) dye from aqueous solution using chemo- physically activated biochar from oil palm empty fruit bunch fiber," *Arabian Journal of Chemistry*, vol. 13, no. 5, pp. 5417–5429, 2020.

[31] X. Pang, L. Sellaoui, D. Franco et al., "Adsorption of crystal violet on biomasses from pecan nutshell, para chestnut husk,

araucaria bark and palm cactus: experimental study and theoretical modeling via monolayer and double layer statistical physics models," *Chemical Engineering Journal*, vol. 378, article 122101, 2019.

[32] H. Xue, X. Gao, M. K. Seliem et al., "Efficient adsorption of anionic azo dyes on porous heterostructured MXene/biomass activated carbon composites: experiments, characterization, and theoretical analysis via advanced statistical physics models," *Chemical Engineering Journal*, vol. 451, article 138735, 2023.

[33] Q. Ge, Q. Tian, M. Moeen, and S. Wang, "Facile synthesis of cauliflower leaves biochar at low temperature in the air atmosphere for Cu (II) and Pb (II) removal from water," *Materials*, vol. 13, no. 14, p. 3163, 2020.

[34] N. Jayan, L. D. Bhatlu, and S. T. Akbar, "Central composite design for adsorption of Pb(II) and Zn(II) metals on PKM-2 *Moringa oleifera* leaves," *ACS Omega*, vol. 6, no. 39, pp. 25277–25298, 2021.

[35] B. B. Mohammed, A. Hsini, Y. Abdellaoui et al., "Fe-ZSM-5 zeolite for efficient removal of basic Fuchsin dye from aqueous solutions: synthesis, characterization and adsorption process optimization using BBD-RSM modeling," *Journal of Environmental Chemical Engineering*, vol. 8, no. 5, article 104419, 2020.

[36] Z. L. Yaneva and N. V. Georgieva, "Insights into Congo Red adsorption on agro-industrial materials- spectral, equilibrium, kinetic, thermodynamic, dynamic and desorption studies. A review," *International Review of Chemical Engineering*, vol. 4, no. 2, pp. 127–146, 2012.

[37] A. E. Ofomaja and E. B. Naidoo, "Biosorption of copper from aqueous solution by chemically activated pine cone: a kinetic study," *Chemical Engineering Journal*, vol. 175, pp. 260–270, 2011.

[38] E. Coates, "Aggregation of dyes in aqueous solutions," *Journal of the Society of Dyers and Colourists*, vol. 85, no. 8, pp. 355–368, 1969.

[39] M. C. Grieve, R. M. Griffin, and R. Malone, "Characteristic dye absorption peaks found in the FTIR spectra of coloured acrylic fibres," *Science & Justice: Journal of the Forensic Science Society*, vol. 38, no. 1, pp. 27–37, 1998.

[40] L. D. Yamil, J. Georgin, D. S. Franco et al., "Powdered biosorbent from pecan pericarp (*Carya illinoensis*) as an efficient material to uptake methyl violet 2B from effluents in batch and column operations," *Advanced Powder Technology*, vol. 31, no. 7, pp. 2843–2852, 2020.

[41] N. El Messaoudi, A. Dbik, M. El Khomri, A. Sabour, S. Bentahar, and A. Lacherai, "Date stones of *Phoenix dactylifera* and jujube shells of *Ziziphus lotus* as potential biosorbents for anionic dye removal," *International Journal of Phytoremediation*, vol. 19, no. 11, pp. 1047–1052, 2017.

[42] T. Siengchum, M. Isenberg, and S. S. C. Chuang, "Fast pyrolysis of coconut biomass - an FTIR study," *Fuel*, vol. 105, pp. 559–565, 2013.

[43] A. H. Jawad and A. S. Abdulhameed, "Statistical modeling of methylene blue dye adsorption by high surface area mesoporous activated carbon from bamboo chip using KOH-assisted thermal activation," *Energy, Ecology and Environment*, vol. 5, no. 6, pp. 456–469, 2020.

[44] N. C. Feng and X. Y. Guo, "Characterisation of adsorptive capacity and mechanisms on adsorption of copper, lead and zinc by modified orange peel," *Transactions of Nonferrous Metals Society of China*, vol. 22, no. 5, pp. 1224–1231, 2012.

[45] V. H. Vargas, R. R. Paveglio, P. D. Pauletto, N. P. Salau, and L. G. Dotto, "Sisal fiber as an alternative and cost-effective adsorbent for the removal of methylene blue and reactive black 5 dyes from aqueous solutions," *Chemical Engineering Communications*, vol. 207, no. 4, pp. 523–536, 2020.

[46] G. Zadora and Z. Brożek-Mucha, "SEM-EDX–a useful tool for forensic examinations," *Materials Chemistry and Physics*, vol. 81, no. 2-3, pp. 345–348, 2003.

[47] N. K. Amin, "Removal of direct blue-106 dye from aqueous solution using new activated carbons developed from pomegranate peel: adsorption equilibrium and kinetics," *Journal of Hazardous Materials*, vol. 165, no. 1-3, pp. 52–62, 2009.

[48] D. Sarkar and A. Bandyopadhyay, "Shrinking core model in characterizing aqueous phase dye adsorption," *Chemical Engineering Research and Design*, vol. 89, no. 1, pp. 69–77, 2011.

[49] O. F. Okeola, *Preparation and characterisation of activated carbon from various waste materials. [Doctoral dissertation, M. Sc. Thesis]*, vol. 5, University of Ilorin, 1999.

[50] A. O. Dada, A. A. Inyinbor, and A. Oluyori, "Comparative adsorption of dyes unto activated carbon prepared from maize stems and sugar cane stems," *Comparative Adsorption of Dyes unto Activated Carbon Prepared from Maize Stems and Sugar Cane Stems*, vol. 2, pp. 38–43, 2012.

[51] E. Yabalak, Ö. Görmez, and A. M. Gizir, "Subcritical water oxidation of propham by H_2O_2 using response surface methodology (RSM)," *Journal of Environmental Science and Health, Part B*, vol. 53, no. 5, pp. 334–339, 2018.

[52] M. Y. Noordin, V. C. Venkatesh, S. Sharif, S. Elting, and A. Abdullah, "Application of response surface methodology in describing the performance of coated carbide tools when turning AISI 1045 steel," *Journal of Materials Processing Technology*, vol. 145, no. 1, pp. 46–58, 2004.

[53] D. Chakraborty, G. Gupta, and B. Kaur, "Metabolic engineering of *E. coli* top 10 for production of vanillin through FA catabolic pathway and bioprocess optimization using RSM," *Protein Expression and Purification*, vol. 128, pp. 123–133, 2016.

[54] P. Nitnithiphrut, M. Thabuot, and V. Seithtanabutara, "Fabrication of composite supercapacitor containing para wood-derived activated carbon and TiO_2," *Energy Procedia*, vol. 138, pp. 116–121, 2017.

[55] J. Jaafari, H. Barzanouni, S. Mazloomi et al., "Effective adsorptive removal of reactive dyes by magnetic chitosan nanoparticles: kinetic, isothermal studies and response surface methodology," *International Journal of Biological Macromolecules*, vol. 164, pp. 344–355, 2020.

[56] R. H. Myers, D. C. Montgomery, and C. M. Anderson-Cook, *Response Surface Methodology: Process and Product Optimisation Using Designed Experiments*, Wiley, Hoboken, New Jersey, Fourth edition edition, 2016.

[57] M. B. Baskan and A. Pala, "A statistical experiment design approach for arsenic removal by coagulation process using aluminum sulfate," *Desalination*, vol. 254, no. 1-3, pp. 42–48, 2010.

[58] R. Kvg, S. Das, J. W. Osborne, C. Natarajan, and A. Mukherjee, "Novel nano-bio (Nano Zerovalent Iron and *Klebsiella* sp.) composite beads for congo red removal using response surface methodology," *Journal of Environmental Chemical Engineering*, vol. 7, no. 5, article 103413, 2019.

[59] N. Aktaş, "Optimization of biopolymerization rate by response surface methodology (RSM)," *Enzyme and Microbial Technology*, vol. 37, no. 4, pp. 441–447, 2005.

[60] S. S. Vieira, Z. M. Magriotis, N. A. Santos, M. das Gracas Cardoso, and A. A. Saczk, "Macauba palm (*Acrocomia aculeata*) cake from biodiesel processing: an efficient and low cost substrate for the adsorption of dyes," *Chemical Engineering Journal*, vol. 183, pp. 152–161, 2012.

[61] Y. M. Slokar and A. Majcen Le Marechal, "Methods of decoloration of textile wastewaters," *Dyes and Pigments*, vol. 37, no. 4, pp. 335–356, 1998.

[62] A. M. Aljeboree, A. N. Alshirifi, and A. F. Alkaim, "Kinetics and equilibrium study for the adsorption of textile dyes on coconut shell activated carbon," *Arabian Journal of Chemistry*, vol. 10, Supplement 2, pp. S3381–S3393, 2017.

[63] R. Lafi, I. Montasser, and A. Hafiane, "Adsorption of Congo red dye from aqueous solutions by prepared activated carbon with oxygen-containing functional groups and its regeneration," *Adsorption Science & Technology*, vol. 37, no. 1-2, pp. 160–181, 2019.

[64] M. Ngabura, S. A. Hussain, W. A. W. Ghani, M. S. Jami, and Y. P. Tan, "Utilization of renewable durian peels for biosorption of zinc from wastewater," *Journal of Environmental Chemical Engineering*, vol. 6, no. 2, pp. 2528–2539, 2018.

[65] M. Özacar and İ. A. Şengil, "Adsorption of reactive dyes on calcined alunite from aqueous solutions," *Journal of Hazardous Materials*, vol. 98, no. 1-3, pp. 211–224, 2003.

[66] A. K. Patil and V. S. Shrivastava, "*Alternanthera bettzichiana* plant powder as low cost adsorbent for removal of Congo red from aqueous solution," *International Journal of ChemTech Research*, vol. 2, no. 2, pp. 842–850, 2010.

[67] Z. Hu, H. Chen, F. Ji, and S. Yuan, "Removal of Congo Red from aqueous solution by cattail root," *Journal of Hazardous Materials*, vol. 73, pp. 292–297, 2010.

[68] N. Rajamohan, "Equilibrium studies on sorption of an anionic dye onto acid-activated water hyacinth roots," *African Journal of Environmental Science and Technology*, vol. 3, no. 11, pp. 399–404, 2009.

[69] R. Venckatesh, T. Amudha, R. Sivaraj, M. Chandramohan, and M. Jambulingam, "Kinetics and equilibrium studies of adsorption of Direct Red-28 onto Punica granatum carbon," *International Journal of Engineering, Science and Technology*, vol. 2, no. 6, pp. 2040–2050, 2010.

[70] M. S. Reddy, L. Sivaramakrishna, and A. V. Reddy, "The use of an agricultural waste material, Jujuba seeds for the removal of anionic dye (Congo red) from aqueous medium," *Journal of Hazardous Materials*, vol. 203, pp. 118–127, 2012.

[71] G. Annadurai, R. S. Juang, and D. J. Lee, "Use of cellulose-based wastes for adsorption of dyes from aqueous solutions," *Journal of Hazardous Materials*, vol. 92, no. 3, pp. 263–274, 2002.

[72] J. Iqbal, N. S. Shah, M. Sayed et al., "Nano-zerovalent manganese/biochar composite for the adsorptive and oxidative removal of Congo-red dye from aqueous solutions," *Journal of Hazardous Materials*, vol. 403, article 123854, 2021.

[73] K. L. Yu, X. J. Lee, H. C. Ong et al., "Adsorptive removal of cationic methylene blue and anionic Congo red dyes using wet-torrefied microalgal biochar: equilibrium, kinetic and mechanism modeling," *Environmental Pollution*, vol. 272, article 115986, 2021.

[74] M. M. Iqbal, M. Imran, T. Hussain et al., "Effective sequestration of Congo red dye with ZnO/cotton stalks biochar nanocomposite: modeling, reusability and stability," *Journal of Saudi Chemical Society*, vol. 25, no. 2, article 101176, 2021.

[75] N. O. Rubangakene, A. Elwardany, M. Fujii, H. Sekiguchi, M. Elkady, and H. Shokry, "Biosorption of Congo Red dye from aqueous solutions using pristine biochar and ZnO biochar from green pea peels," *Chemical Engineering Research and Design*, vol. 189, pp. 636–651, 2023.

[76] S. K. Lagergren, "About the theory of so-called adsorption of soluble substances," *Sven. Vetenskapsakad. Handingarl*, vol. 24, pp. 1–39, 1898.

[77] S. Canzano, P. Iovino, V. Leone, S. Salvestrini, and S. Capasso, "Use and misuse of sorption kinetic data: a common mistake that should be avoided," *Adsorption Science & Technology*, vol. 30, no. 3, pp. 217–225, 2012.

[78] Y. S. Ho and G. McKay, "Pseudo-second order model for sorption processes," *Process Biochemistry*, vol. 34, no. 5, pp. 451–465, 1999.

[79] S. Roginsky and Y. B. Zeldovich, "The catalytic oxidation of carbon monoxide on manganese dioxide," *Acta physicochimica U.R.S.S*, vol. 1, no. 554, p. 2019, 1934.

[80] W. J. Weber Jr. and J. C. Morris, "Kinetics of adsorption on carbon from solution," *Journal of the Sanitary Engineering Division*, vol. 89, pp. 31–59, 1963.

[81] S. Zafar, N. Khalid, M. Daud, and M. L. Mirza, "Kinetic studies of the adsorption of thorium ions onto rice husk from aqueous media: linear and nonlinear approach," *The Nucleus*, vol. 52, no. 1, pp. 14–19, 2015.

[82] J. Lin and L. Wang, "Comparison between linear and non-linear forms of pseudo-first-order and pseudo-second-order adsorption kinetic models for the removal of methylene blue by activated carbon," *Frontiers of Environmental Science & Engineering in China*, vol. 3, no. 3, pp. 320–324, 2009.

[83] G. C. Panda, S. K. Das, and A. K. Guha, "Jute stick powder as a potential biomass for the removal of Congo red and rhodamine B from their aqueous solution," *Journal of Hazardous Materials*, vol. 164, no. 1, pp. 374–379, 2009.

[84] Y. Fan, H. J. Liu, Y. Zhang, and Y. Chen, "Adsorption of anionic MO or cationic MB from MO/MB mixture using polyacrylonitrile fiber hydrothermally treated with hyperbranched polyethylenimine," *Journal of Hazardous Materials*, vol. 283, pp. 321–328, 2015.

[85] C. Namasivayam and D. Kavitha, "Removal of Congo Red from water by adsorption onto activated carbon prepared from coir pith, an agricultural solid waste," *Dyes and Pigments*, vol. 54, no. 1, pp. 47–58, 2002.

[86] D. Appala Naidu, P. Vijay, P. King, and V. S. Prasad, "Biosorption of Congo red from aqueous solution using guava (Psidium Guajava) leaf powder: equilibrium and kinetic studies," *The IUP Journal of Chemical Engineering*, vol. 2, no. 1, pp. 27–45, 2010.

[87] N. Hoda, E. Bayram, and E. Ayranci, "Kinetic and equilibrium studies on the removal of acid dyes from aqueous solutions by adsorption onto activated carbon cloth," *Journal of Hazardous Materials*, vol. 137, no. 1, pp. 344–351, 2006.

[88] R. Wu, J. Qu, and Y. Chen, "Magnetic powder MnO-Fe_2O_3 composite–a novel material for the removal of azo-dye from water," *Water Research*, vol. 39, no. 4, pp. 630–638, 2005.

[89] J. M. Jabar, Y. A. Odusote, K. A. Alabi, and I. B. Ahmed, "Kinetics and mechanisms of Congo-red dye removal from aqueous solution using activated *Moringa oleifera* seed coat as adsorbent," *Applied Water Science*, vol. 10, no. 6, pp. 1–11, 2020.

[90] M. A. Adebayo, J. M. Jabar, J. S. Amoko, E. O. Openiyi, and O. O. Shodiya, "Coconut husk-raw clay-Fe composite: preparation, characteristics and mechanisms of Congo red adsorption," *Scientific Reports*, vol. 12, no. 1, p. 14370, 2022.

[91] J. M. Jabar, M. A. Adebayo, I. A. Owokotomo, Y. A. Odusote, and M. Yılmaz, "Synthesis of high surface area mesoporous $ZnCl_2$-activated cocoa (*Theobroma cacao* L) leaves biochar derived *via* pyrolysis for crystal violet dye removal," *Heliyon*, vol. 8, no. 10, article e10873, 2022.

[92] M. I. Din, Z. Hussain, M. L. Mirza, A. T. Shah, and M. M. Athar, "Adsorption optimization of lead (II) using *Saccharum bengalense* as a non-conventional low cost biosorbent: isotherm and thermodynamics modeling," *International Journal of Phytoremediation*, vol. 16, no. 9, pp. 889–908, 2014.

[93] P. V. Nidheesh, R. Gandhimathi, S. T. Ramesh, and T. S. A. Singh, "Adsorption and desorption characteristics of crystal violet in bottom ash column," *Journal of Urban and Environmental Engineering*, vol. 6, no. 1, pp. 18–29, 2012.

[94] R. S. Blackburn, "Natural polysaccharides and their interactions with dye molecules: application in effluent treatment," *Environmental Science & Technology*, vol. 2004, no. 38, pp. 4905–4909, 2004.

[95] I. D. Mall, V. C. Srivastava, N. K. Agarwal, and I. M. Mishra, "Removal of Congo red from aqueous solution by bagasse fly ash and activated carbon: kinetic study and equilibrium isotherm analyses," *Chemosphere*, vol. 61, no. 4, pp. 492–501, 2005.